SEB SOCIETY FOR EXPERIMENTAL BIOLOGY

Journal of Experimental Botany, Vol. 74, No. 18 pp. 5458–5471, 2023
https://doi.org/10.1093/jxb/erad252 Advance Access Publication 6 July 2023

Journal of Experimental Botany

EXPERT VIEW

New foundations for the physical mechanism of variable chlorophyll *a* fluorescence. Quantum efficiency versus the light-adapted state of photosystem II

Győző Garab[1,2,*], Melinda Magyar[1], Gábor Sipka[1] and Petar H. Lambrev[1]

[1] Institute of Plant Biology, Biological Research Centre, Szeged, Hungary
[2] Department of Physics, Faculty of Science, University of Ostrava, Ostrava, Czech Republic

[*] Correspondence: garab.gyozo@brc.hu

Received 23 May 2023; Editorial decision 26 June 2023; Accepted 3 July 2023

Editor: Karl-Josef Dietz, Bielefeld University, Germany

Abstract

Photosystem II (PSII) uses solar energy to oxidize water and delivers electrons to fix CO_2. Although the structure at atomic resolution and the basic photophysical and photochemical functions of PSII are well understood, many important questions remain. The activity of PSII *in vitro* and *in vivo* is routinely monitored by recording the induction kinetics of chlorophyll *a* fluorescence (ChlF). According to the 'mainstream' model, the rise from the minimum level (F_o) to the maximum (F_m) of ChlF of dark-adapted PSII reflects the closure of all functionally active reaction centers, and the F_v/F_m ratio is equated with the maximum photochemical quantum yield of PSII (where $F_v=F_m-F_o$). However, this model has never been free of controversies. Recent experimental data from a number of studies have confirmed that the first single-turnover saturating flash (STSF), which generates the closed state ($PSII_C$), produces $F_1<F_m$, and have uncovered rate-limiting steps ($\Delta\tau_{1/2}$ half-waiting times) in the multi-STSF-induced F_1-to-F_m increments that originate from the gradual formation of light-adapted charge-separated states ($PSII_L$) with significantly increased stability of charges compared to the $PSII_C$ state that is elicited by a single STSF. All the data show that the interpretation of ChlF must be laid on new foundations. Here, we discuss the underlying physical mechanisms and the significance of structural/functional dynamics of PSII as reflected by ChlF and variations in the novel parameter $\Delta\tau_{1/2}$.

Keywords: Chlorophyll *a* fluorescence induction, conformational changes, dielectric relaxation, electric field effects, F_v/F_m, light-adapted charge-separated state, photosystem II, photochemical quantum efficiency, purple bacterial reaction center, Q_A-model.

Introduction

Photosystem II (PSII), or water-plastoquinone oxidoreductase, uses light energy to oxidize water, thereby providing us with an oxygenic atmosphere and, in concert with photosystem I (PSI), delivers electrons for the conversion of carbon dioxide to sugars. PSII is the engine of life: it is the ultimate source of virtually all reducing equivalents in the biosphere (Barber, 2004). PSII is probably the most-studied light-induced enzyme, and its crystal structure and basic photophysical and photochemical functions are reasonably well understood (Coe *et al.*, 2015; Nelson and Junge, 2015; Shen, 2015; Romero *et al.*, 2017; Shevela *et al.*, 2023).

PSII is a large, multi-subunit homodimeric protein complex that is embedded in the thylakoid membranes of cyanobacteria, algae, and vascular plants. The smallest fully functional unit of PSII is the core complex (CC), found in cyanobacteria, which has a molecular mass of ~700 kDa. Each monomer of the dimeric PSII CC contains the reaction center (RC) incorporated in the D1/D2 proteins, the α and ß subunits of cytochrome b_{559}, the two core antenna proteins CP43 and CP47, which mostly carry 13 and 16 chlorophyll *a* (Chl *a*) molecules, respectively, the oxygen-evolving complex (OEC) containing the Mn_4CaO_5 cluster, and additional proteins (Umena *et al.*, 2011; Suga *et al.*, 2019; Shevela *et al.*, 2023). PSII CCs in green algae and land plants are associated with large, membrane-intrinsic, light-harvesting antenna systems that are constituted by minor and major light-harvesting antenna complexes (LHCII), which considerably extend the absorption cross-section of PSII and which supply additional excitation energy—via the core antenna complexes—to the RC. These peripheral antenna complexes are capable of switching between light-harvesting at low light and dissipation of excitation-energy in excess light, and thus they participate in regulatory processes and in the photoprotection of the photosynthetic machinery (Horton, 2012; Croce and van Amerongen, 2014; Ruban and Wilson, 2021).

The co-factor structure of the RC of PSII and the routes of charge separation and approximate electron-transfer time constants are shown in Fig. 1. The RC complex of PSII contains four Chls (the two accessory Chls Chl_{D1} and Chl_{D2}, and the Chl *a* molecules P_{D1} and P_{D2}), two pheophytins ($Pheo_{D1}$ and $Pheo_{D2}$), and the two plastoquinone molecules Q_A and Q_B, which are the first and second stable electron acceptors, respectively. On the donor side, the redox-active tyrosine residues Y_Z and Y_D are accommodated by the D1/D2 proteins; the assembly and activity of the OEC is linked to the core antenna protein CP43 (Fig. 1A) (Barber *et al.*, 2000; Shen, 2015; Zabret *et al.*, 2021).

In the functional, open-state of PSII ($PSII_O$) when it is capable of generating stable charge separation, upon direct excitation of the RC complex or upon the arrival of an exciton, charge separation occurs that proceeds asymmetrically along the D1 branch on a timescale of ps with the formation of $P_{680}^{\bullet+}Pheo^{\bullet-}$. It should be noted that the molecular identity of the primary donor–acceptor pair is still under debate and can even vary (Novoderezhkin *et al.*, 2011; Muh *et al.*, 2017), and hereafter we denote the primary electron donor as P_{680}, which according to Shevela *et al.* (2023) is an ensemble of four Chls *a*, namely $Chl_{D1}/P_{D1}/P_{D2}/Chl_{D2}$. The charge separation is stabilized by the re-oxidation of $Pheo^{\bullet-}$ by Q_A, which occurs on a timescale of ~300 ps (Fig. 1B). The primary electron donor is then re-reduced (timescale tens of ns) by electron donation from the nearby redox-active tyrosine, forming the neutral tyrosyl radical $Y_Z^{\bullet}(H^+)$, which is then reduced by the Mn_4CaO_5 cluster, leading to the $S_2^{(+)}$ state of the OEC; this proceeds at a timescale of tens of μs. The stabilization of the charge-separated state generates $PSII_C$, the closed state of PSII with Q_A reduced. This state persists for several hundreds of μs until the electron is transferred from Q_A to Q_B, a process with strong temperature dependence (Shlyk-Kerner *et al.*, 2006); a charge separation following the re-opening of the RC is accompanied by the advancement of the S-states of the OEC. The secondary electron transfer step in PSII from Q_A to Q_B, which re-opens $PSII_C$, can be blocked by PSII inhibitor molecules such as DCMU [*N′*-(3,4-dichlorophenyl)-*N*,*N*-dimethylurea], or by the full

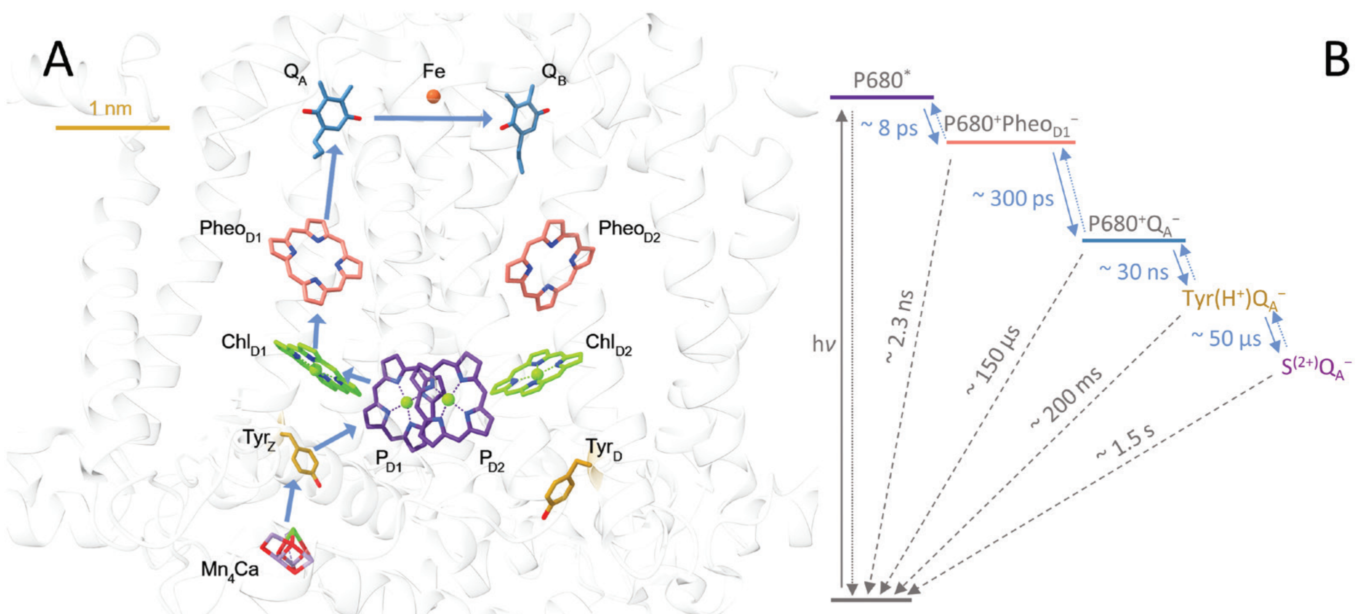

Fig. 1. The photosystem II reaction center of *Thermosynechococcus vulcanus* (pdb:5GTH). (A) Co-factor structure and (B) the routes of charge separation and approximate electron transfer and back reaction time constants (based on data from Cser and Vass (2007) from *Synechocystis* 6803). The structure is visualized using UCSF ChimeraX (Pettersen *et al.*, 2021).

Box 1. ChlF induction kinetics, the Q_A model, quantum efficiency, and controversies

- **Basic observations**

Dark-adapted open-state PSIIs, with all Q_A in oxidized state, display the minimal fluorescence level, F_o (or O). Upon an intense rectangular-profile excitation of PSII in the presence of DCMU, the RCs close and the fluorescence rapidly rises to the maximal level, F_m (P). In samples possessing active whole-chain electron transport, the light-induced rise in Chl *a* fluorescence is more complex. It starts with a fast (~2 ms) O-to-J rise phase, which is known as the photochemical phase; the much slower J–I and I–P steps, which are linked to the linear electron transport activity all the way to the PSI acceptor side (Schansker *et al.*, 2005), are traditionally considered as thermal phases, at the end of which (in less than ~1 s) F_m (P) is reached (Morin, 1964; Delosme, 1967; Stirbet and Govindjee, 2011). Direct contributions from PSI to the F_o and F_m levels are usually small, albeit they might not be negligible (Campbell *et al.*, 1998; Schreiber, 2023). In the following sections, we focus our attention on ChlF from PSII.

- **The Q_A model of ChlF**

According to the 'classical' or 'mainstream' model, the ChlF transients reflect the kinetics of the reduction of Q_A: 'to reach F_m, it is necessary, and sufficient, to have Q_A completely reduced in all the active PSII centers' (Stirbet and Govindjee, 2012). This, the so-called Q_A model of ChlF, is based on the model of Duysens and Sweers (1963) and assumes that the RCs of PSII exist in two states, quenched and unquenched, containing oxidized and reduced quenchers (Q and QH; corresponding to Q_A and Q_A^-, respectively).

- **Determination of the photochemical quantum yield of PSII using the F_v/F_m ratio**

The Q_A model paved the way for determining the maximum quantum efficiency of PSII via measuring the F_o and F_m levels and calculating the F_v/F_m ratio (where F_v=F_m–F_o). Indeed, in most plant biology textbooks and manuals of ChlF devices, the F_v/F_m ratio for dark-adapted samples is equated with the maximum quantum yield of PSII. This is based on the correlation that the fate of absorbed photons has three pathways, namely photochemistry (p), fluorescence (f), and dissipation (d) and that the total yield of these processes is always 1, which was first recognized by Butler (1978). In the following, we adopt the notation used by Blankenship (2021), and *d* is used to include all other routes.

As explained by Blankenship (2021), with parallel first-order reactions in which each process displays its exponential decay characterized by a rate constant *k*, the overall decay of the initial state (*A*) can be described with the help of the sum of the k_i rate constants (k_Σ, representing the observed k_{obs}); and thus, *A* decays exponentially with k_{obs}. Accordingly, the fractional yield of process *i* (Y_i) can be given as

$$Y_i = \frac{k_i}{k_\Sigma}. \tag{1}$$

Using these basic correlations and the rate constants given for $PSII_O$ (open) and $PSII_C$ (closed), which—according to the Q_A model—produce the F_o and F_m levels, respectively, the following expressions are obtained:

$$F_o = \frac{k_f}{k_f + k_p + k_d}, \tag{2}$$

and

$$F_m = \frac{k_f}{k_f + k_d}, \tag{3}$$

and thus:

$$\frac{F_v}{F_m} = \frac{k_p}{k_f + k_d} = Y_p. \tag{4}$$

Conventionally, Y_p is denoted as φ_{Po} (Strasser *et al.*, 2004).

- **Controversies: the main problems with the Q_A model**

Despite the immense success of the use of ChlF in plant biology, by the 1960s and 1970s there were already controversies concerning the Q_A model, and they have continued to persist and indeed grow in number to this day.

One of the crucial problems that emerged early was that in intact photosynthetic organisms, F_m could not be reached despite the notion that the photochemical phase was completed by intense rectangular-profile excitations (Delosme, 1967). In fact, the O–J phase never reached F_m although each PSII was excited multiple times in the first ~2 ms: simple calculations have shown that at a photon flux density of 3000 μmol m^{-2} s^{-1} each PSII becomes excited once every ~200 μs (cf. Neubauer and Schreiber, 1987; Lazár and Pospíšil, 1999), but P was not reached even with a photon flux density of 15 000 μmol m^{-2} s^{-1} (Schansker *et al.*, 2011). Further, Joliot and Joliot (1979), using isolated thylakoid membranes in the presence of DCMU, demonstrated that whereas the formation of a charge-separated state in PSII was completed by a single-turnover saturating flash (STSF), ChlF was not saturated. In particular, it was shown that the first STSF induced a fluorescence level (hereafter named F_1) that was significantly lower than F_m, and to reach F_m a train of additional STSFs were required; however, these generated no additional stable charge separation. To resolve this discrepancy within the framework of the Q_A model, the authors hypothesized the presence of a second quencher (named Q_2), which was suggested to act after the full reduction of Q_1 (Q_A). It should be noted that in hindsight—with the benefit of structural data that only became available much later—Pierre Joliot would have sought a different explanation (personal communication to one of us, GG).

An additional controversy is that the rise kinetics of ChlF in the presence of DCMU follow a sigmoidal pattern rather than the expected exponential one. This non-linearity is explained by the excitonic connectivity of PSII units, namely the transfer of the excitation energy from a $PSII_C$ to a nearby $PSII_O$ (see Stirbet, 2013). In this context, it is interesting to recall the data of France *et al.* (1992), who found that both the magnitude and the shape of the flash-induced ChlF depended on the length of the 2–50 μs long flashes that they applied, which contained the same amount of quanta—revealing a complex dependence of the computed connectivity parameter on the distribution of the exciting quanta, and its dependence on single-turnover (2 μs) versus multiple turnover (50 μs) excitations. The authors ascribed these pulse length-dependent changes to variations in the connectivity of PSII units, but noted that the basic phenomena underlying their observations needed to be investigated further. It is also important to mention here that, as pointed out by Vredenberg (2008), sigmoidicity might arise from overlapping exponential kinetic components.

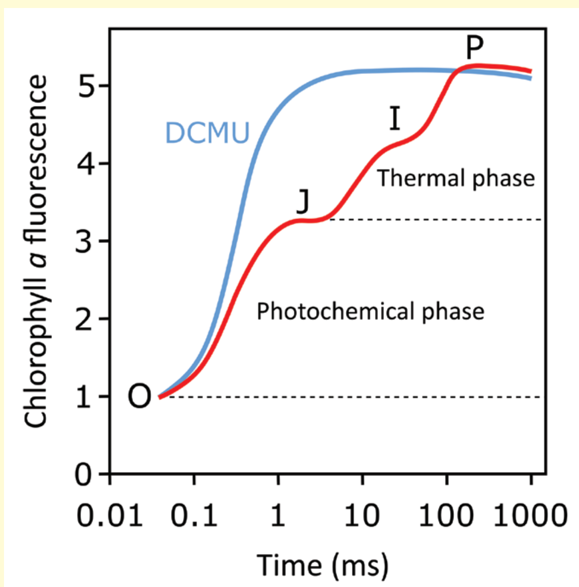

Fast Chl-*a* fluorescence transients at room temperature of a control and a DCMU-treated pea leaf. Modified from Stirbet and Govindjee (2011), with permission from Elsevier.

pre-reduction of the plastoquinone pool, which can occur for example in leaves under anaerobiotic conditions (Tóth *et al.*, 2007). Under these conditions, $PSII_C$ can assume a stationary state, determined only by the thermally assisted charge recombination between Q_A^- and $S_2^{(+)}$ (Tyystjarvi and Vass, 2004).

Monitoring the activity of PSII using the induction of chlorophyll *a* fluorescence

The activity of PSII—at the different levels of structural complexity from isolated CCs or thylakoid membranes to whole plants and phytoplankton communities—is routinely monitored by using the technique of Chl *a* fluorescence (ChlF) induction kinetics (Papageorgiou and Govindjee, 2004; Strasser *et al.*, 2004; Gorbunov and Falkowski, 2022). The dark-to-light transition of PSII is characterized either by variations in the yield or the intensity of the fluorescence emission, during which the fluorescence yield rises from F_o to F_m, and the intensity rises from O to P (Box 1).

As well as typical ChlF induction curves, Box 1 also describes the interpretation of these transients within the framework of the 'mainstream' or so-called Q_A model, and it highlights the main controversial features of this.

Several additional controversial features have been found by different authors, with all of the findings demonstrating the complexity of ChlF and suggesting complementary interpretations beyond the Q_A model (Moise and Moya, 2004; Schansker *et al.*, 2011; Kalaji *et al.*, 2014; Vredenberg, 2015; Treves *et al.*, 2016). The controversies, combined with the overwhelming success of the use of ChlF techniques in characterizing (at least phenomenologically) photosynthetic functions at virtually all scales of complexity (Papageorgiou and Govindjee, 2004), in fingerprinting different mutants and the effects of biotic and abiotic stresses (Yao *et al.*, 2018), and in portraying large land and marine ecosystems (Gorbunov and Falkowski, 2022; Loayza *et al.*, 2023), have inspired further research in different laboratories to better understand the dark-to-light transition in PSII. Recent experiments have revealed some unexpected features of F_v and of PSII RC states, and provided irrevocable evidence that the Q_A model is incorrect (Box 2).

The F_v/F_m parameter cannot be equated with the quantum efficiency of PSII

Based on the findings listed in Box 2, it is clear that the F_v/F_m parameter cannot and should not be equated with the quantum efficiency of PSII, and that the basic postulations of the Q_A model need reconsideration. In the following sections, we show that, indeed, fundamental implicit assumptions involved in the calculation of the maximum quantum yield of PSII (Y_p; commonly denoted as φ_{Po}) cannot be justified; further, the reduction of Q_A causes only a minor rise in ChlF.

When using the equations related to the calculated value of Y_p (Box 1), as based on the F_v/F_m parameter, it is important to recognize the implicit assumptions that 'none of the rate constants change as the traps go from open to closed, and that all the fluorescence that is observed in both the F_o and F_m states come from a homogeneous system in which all chlorophyll excited states are equivalent' (Blankenship, 2021). In intact systems, variable degrees of PSI or antenna contributions (Campbell *et al.*, 1998; Santabarbara *et al.*, 2019), non-photochemical quenching and state transitions (Oxborough and Baker, 1997; Maxwell and Johnson, 2000; Horton, 2012; Murchie and Harbinson, 2014; Ruban and Wilson, 2021) might complicate the picture; these evidently limit the applicability of the Q_A model. However, even in the simplest case in isolated PSII CCs, the assumptions are not justifiable. For example, under F_o, F_1, and F_m conditions, the decay kinetics cannot be described by single exponentials (Sipka *et al.* (2021); for F_m see also Szczepaniak *et al.* (2009), Caffarri *et al.* (2011), Miloslavina *et al.* (2006) and van der Weij-de Wit *et al.* (2011). On the contrary, instead of a homogenous pigment system, the data presently available and theoretical models suggest a high complexity of processes beyond the emission of fluorescence, determined by a range of different rate constants in the excitation energy and electron-transfer pathways (Shibata *et al.*, 2013; Yang *et al.*, 2022). In addition, spectrally-resolved single-turnover saturating flash (STSF-)induced ChlF transients of the PSII CC at 80 K have shown that the intensity ratio of the two main emission bands—F_{685} and F_{695}, arising from CP43 and CP47, respectively—changes dramatically during the induction, with most prominent intensity and spectral changes occurring between $PSII_C$ and $PSII_L$ (Sipka *et al.*, 2021). In addition, and most importantly, the rate constants change between $PSII_C$ and $PSII_L$, as evidenced by Chl *a* spectral and lifetime measurements on DCMU-treated PSII CCs under (or near to) F_1 and F_m conditions at 5 °C (Sipka *et al.*, 2021).

Hence, instead of Equations 2 and 3 in Box 1, we should write:

$$F_o = \frac{k_{fo}}{k_{fo} + k_{po} + k_{do}}, \tag{5}$$

and

$$F_m = \frac{k_{fm}}{k_{fm} + k_{dm}}. \tag{6}$$

Here, the second indices (o and m) refer to the actual ChlF levels. It is evident that combining these equations and calculating the F_v/F_m ratio would hardly provide any easily interpretable physical meaning of this parameter.

It must also be pointed out that the above equations do not yield realistic values for the quantum yield of PSII even if we were to apply them to the $PSII_O$ (F_o) and $PSII_C$ (F_1) states,

Box 2. Key recent developments concerning ChlF and the physiological states of PSII

Until recently, no explanations could be offered for the following perplexing questions. (i) How and why is it that F_m cannot be reached by a short, intense light pulse that closes all the RCs of PSII? (ii) Why do the magnitude and shape of the rise in fluorescence depend on the length of the exciting flash? (iii) Why do the F_1-to-F_m increments require additional flash excitations? And (iv), are there waiting times between the consecutive STSFs that generate the fluorescence increments and, if so, how long are they?

These questions can now be answered; however, this has consequences for the validity of the Q_A model and on conclusions based upon it.

- **Rate-limiting steps associated with ChlF of $PSII_C$: the requirement of waiting times between consecutive STSFs to produce sizeable ChlF increments**

Using a variety of DCMU-treated samples, Magyar *et al*. (2018) discovered that to reach the (quasi-stationary) level of F_2 (and further, F_3, F_4, and finally F_m), a sufficiently long $\Delta\tau_{1/2}$ half-waiting time (in the range of several hundred μs to 1 or 2 ms) had to be employed between two consecutive flashes. The strikingly different temperature-dependences of the incremental rise and of the dark-decay kinetics of ChlF that have been recorded between –100 °C and 25 °C have clearly shown that the single-step F_o-to-F_1 ($PSII_O$-to-$PSII_C$) transient and the gradually generated F_1-to-F_m increments originate from two physically distinct processes. The relatively long $\Delta\tau_{1/2}$ values, which at non-cryogenic temperatures are comparable with the reopening of the RC via Q_A-to-Q_B electron transfer, qualitatively explain why the O–J rise cannot reach P. Furthermore, experiments on isolated PSII CC dimers (Magyar *et al.*, 2018) and monomers (Sipka *et al.*, 2021) revealed that the sigmoidicity of ChlF does not require connectivity between PSII units, and thus arises from overlapping exponential rises (cf. Vredenberg, 2008), from several consecutive light-induced processes from F_i–F_{i+1} rises (i=1, 2, 3 …). These observations do not rule out energetic connectivity, for example between the monomers of a PSII dimer or between the dimer of dimers: the occurrence of energy transfer between monomers has been inferred from femtosecond transient absorption spectroscopy of monomeric and dimeric PSII CCs (Yoneda *et al.*, 2016).

- **The rate-limiting steps do not gate the formation of the primary radical pair**

By employing absorbance transient spectroscopy at 819 nm on DCMU-treated cyanobacterial PSII CCs, Sipka *et al*. (2019) have shown that the formation of $P_{680}{}^{\bullet+}Pheo^{\bullet-}$ primary radical pairs induced by the second and consecutive STSFs are followed by rapid (~2 ns) charge recombinations. This confirms the lack of additional stable charge-separation in $PSII_C$ and suggests that the F_1-to-F_m increments in $PSII_C$ are driven by the intense transient electric field generated by the primary radical pair, and/or might be assisted by dissipative thermal jumps arising from charge recombination.

- **ChlF of $PSII_C$ in untreated leaves of vascular plants**

Using intact leaves, Laisk and Oja (2020) have shown that the 'fluorescence yield of [$PSII_C$] increases during a low to high light induction—while the membrane gets energized and the plastoquinone pool gets reduced'. This finding was explained by a mechanism according to which the transmembrane electric field facilitates the return of the excitation energy from the $P_{680}{}^{\bullet+}Pheo^{\bullet-}$ radical pair to the antenna.

- **The fast ChlF rise following the $PSII_O$-to-$PSII_C$ transition, and the absence of PSII connectivity in leaves**

Using intact leaves of vascular plants, Oja and Laisk (2020) also determined the magnitude of the 'immediate' rise of ChlF after the closure of PSII, and found it to be merely $1.8F_o$; in 40 μs the level increased to $3F_o$, approaching the flash fluorescence yield F_f (F_1) = $0.6F_m$. Kinetic analyses proved the absence of excitonic connectivity between PSII units in leaves, corroborating the conclusions of Magyar *et al.* (2018) who used isolated PSII CCs.

- **The light-adapted charge-separated state ($PSII_L$) with increased stability of the charges, and the distinct and complex de-excitation kinetics of the F_o, F_1, and F_m states**

Sipka *et al*. (2021) revealed the formation of a light-adapted charge-separated state ($PSII_L$) by using DCMU-treated PSII CCs of *Thermosynechococcus vulcanus* and a range of biophysical techniques, including measurements of fluorescence lifetime either at or near to F_o, F_1, and F_m conditions, 80 K emission spectroscopy of ChlF induction, single and multiple STSF-induced rapid-scan FTIR transient spectroscopy, and C550 absorbance transients. The charge-separated state of $PSII_L$ was shown to be substantially stabilized when compared to $PSII_C$; furthermore, $PSII_L$ displayed distinct features in the energy landscape of the trapping/de-trapping of excitations in the core-antenna–reaction center complex. Model calculations strongly suggested the roles of strong local stationary ($Q_A^-S_2^{(+)}$) and transient ($P_{680}^{\bullet+}Pheo^{\bullet-}$) electric fields and dielectric relaxation processes, possibly combined with thermal jumps due to heat dissipation (Cseh *et al.*, 2000), during the $PSII_C$-to-$PSII_L$ transition. It should also be noted here that hydrated biological macromolecules exhibit complex, multicomponent dielectric relaxation processes (Nakanishi and Sokolov, 2015).

- **Lipid dependence of the rate-limiting steps of the $PSII_C$-to-$PSII_L$ transition**

Magyar *et al*. (2022) established that the rate-limiting step of ChlF in DCMU-treated PSII CCs of *T. vulcanus* and spinach thylakoid membranes depended on the lipid content of the samples. The $\Delta\tau_{1/2}$ half-waiting time that characterized the $PSII_C$-to-$PSII_L$ transition was considerably longer in PSII CC than in the thylakoid membranes, but the transition could be accelerated by adding thylakoid lipids to the PSII CC samples.

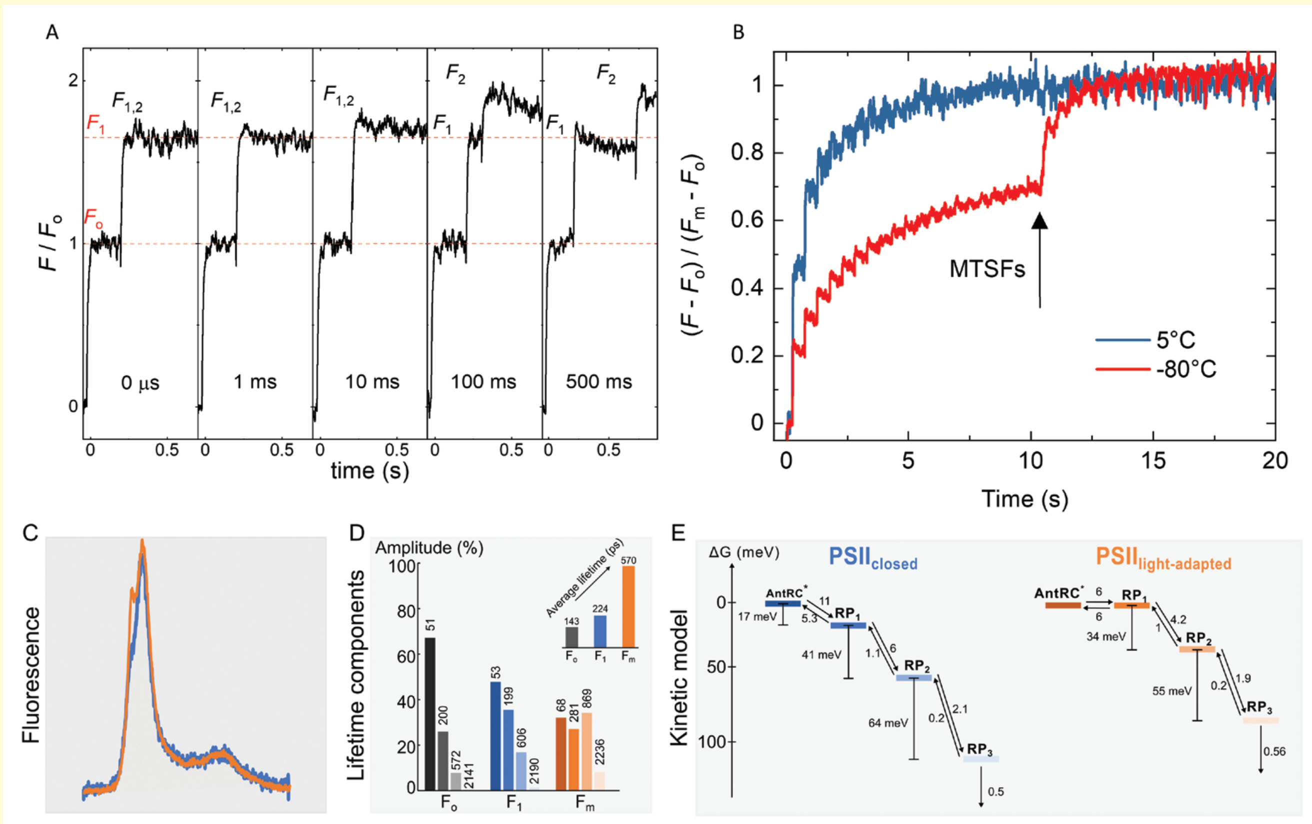

The main novel features of ChlF. (A, B) STSF-induced kinetic transients, as described by Magyar *et al.* (2023). (A) Double-STSFs with different waiting times between the two flashes (as indicated) induce ChlF increments at –80 °C. (B) Transients induced by a train of STSFs followed by multiple-turnover saturating flashes (MTSFs) at either 5 °C or –80 °C. (C, D) Emission spectra and lifetime components of DCMU-treated PSII CCs of *T. vulcanus*, as described by Sipka *et al.* (2021). (C) Normalized 80 K emission spectra. (D) Lifetime components at 5 °C, which are characteristic of the F_o ($PSII_O$, black and grey), F_1 ($PSII_C$, blue colors), and F_m ($PSII_L$, red colors) states. (E) A kinetic model of closed and light-adapted PSII as proposed by Sipka *et al.* (2021).

although the differences in the rate constants are smaller between $PSII_O$ and $PSII_C$ than between $PSII_O$ and $PSII_L$ (Sipka *et al.*, 2021). Evidently, the calculated values of $Y_{p1} = (F_1 - F_o)/F_1$ would be smaller than those of Y_p because $F_1 < F_m$ at all temperatures; thus, neither Y_{p1} nor F_v/F_m is suited as a 'proxy' for Y_p of PSII. Indeed, using published data on samples exhibiting F_v/F_m values ≥0.8, we would obtain Y_{p1} values of 0.76 in DCMU-treated PSII CCs at 5 °C Sipka *et al.* (2019) and 0.4

Box 3. Physical mechanism(s) in Type-II RCs: donor-side modulation of PSII ChlF

It has recently been recognized that when seeking the physical mechanisms that might explain the most peculiar features of the $PSII_C$-to-$PSII_L$ transition, the well-characterized behavior of its ancestor, the purple bacterial RC (bRC), might be of great help (Sipka *et al.*, 2022). PSII RCs and the bRC belong to the Type-II RCs, and have highly similar chromophoric systems and arrangements of the quinone acceptors (Cardona *et al.*, 2012).

• The light-induced RC_C-to-RC_L transition: stabilization of the charge separation

In bRCs, it has been well documented that continued illumination of a closed RC (RC_C) induces substantial stabilization of its charge-separated state, as reflected by increased recombination lifetimes of ~100-times or more of the oxidized primary donor (P^+) and Q_A^-(Goushcha *et al.*, 1999, 2003; Andréasson and Andréasson, 2003; Deshmukh *et al.*, 2011; Malferrari *et al.*, 2013). Earlier observations of Kleinfeld *et al.* (1984) indicated slow structural motions and structural 'memory' effects that were attributed to the formation of light-adapted conformations. Theoretical studies explained this type of behavior of bRCs with a more general self-regulatory mechanism of photoactivated donor–acceptor molecular systems that possess the ability to undergo slow structural reorganization (Goushcha *et al.*, 2000; Christophorov *et al.*, 2003). This theory predicted the gradual formation of a light-adapted conformational state from the dark-adapted conformation of the bRC, induced after repeated excitation of the sample—a behavior that is very similar to the observations related to the transition of $PSII_C$ to $PSII_L$ (Sipka *et al.*, 2021).

• Multiple-step dielectric relaxation processes

Malferrari *et al.* (2013) have proposed that, in line with Marcus' theory (Marcus and Sutin, 1985), the slow conformational changes originate from dielectric relaxation processes following the generation of strong local electric fields, suggesting that the protein matrices of bRC and PSII assume the optimum dielectric environment relatively slowly and only gradually, and that they evidently require the assistance of additional excitations (for further explanation and references, see Sipka *et al.*, 2022). In PSII, the formation of the transient field due to the generation of the primary radical pair $P_{680}^{\bullet+}Pheo^{\bullet-}$, which is superimposed on the quasi-stationary field of $S_2^{(+)}Q_A^-$, is thought to perturb the dielectric matrix and to facilitate, perhaps in combination with the dissipated heat (Cseh *et al.*, 2000), the gradual optimization of the dielectric matrix of the RC, via gradually shielding the charges (Sipka *et al.*, 2021). The transitions might be hindered by the rigidity of the RCs, as indicated by the marked dependence of the recombination rate on the water content of bRCs (Malferrari *et al.*, 2013), and in PSII by the strong temperature-dependences of the F_1 amplitude, the relaxation of F_m, and the magnitude of the half-waiting time $\Delta\tau_{1/2}$ (Magyar *et al.*, 2023). It is also noteworthy that the magnitude of $\Delta\tau_{1/2}$ does not vary along with F_v, i.e. the half-waiting times do not vary during the train of STSFs. Essentially the same $\Delta\tau_{1/2}$ values are obtained between F_i and F_{i+1} for all i=1–4; this is true not only at 5 °C but also at –80 °C, where $\Delta\tau_{1/2}$ is much longer. These data strongly suggest the involvement of the same physical mechanism in the F_1-to-F_m increments (Magyar *et al.*, 2018; Sipka *et al.*, 2021). Transmembrane or external electric fields (which are much less intense compared to local fields) have previously been proposed to play roles in the stabilization of the charges in PSII (Knox and Garab, 1982; Dau and Sauer, 1992; Vredenberg, 2011).

• Hydrogen-bond networks in bRC and PSII RC, and multicomponent modulation of ChlF on the donor side of PSII

The long-lived $P^+Q_A^-$ state in bRCs has recently been shown to be linked to the proton release capability of a hydrogen-bond network that is formed by amino acid residues and bound water molecules near P (Allen *et al.*, 2023). These regions, and similar networks in PSII, are proposed to be involved in the polarization of the RC matrix and thus in the dielectric relaxation processes (Sipka *et al.*, 2022). Electron-transfer reactions of the two redox-active tyrosines have been shown to be coordinated with proton transfer steps (Diner *et al.*, 2004; Nakamura and Noguchi, 2015; Ahmadova *et al.*, 2017), suggesting the role of this region in the gradual formation of $PSII_L$ with a mechanism similar to that in the bRC. Sipka *et al.* (2022) evoked two key factors that had been shown to modulate ChlF on the donor side: (i) the period four oscillation of the fluorescence yield, which indicates a strong S-state dependence of ChlF, both in the presence and absence of Q_A^- (Delosme and Joliot, 2002); and (ii) mutations in the D_2-loop that suppress F_v to 10–15% of that in the control PSI-*minus* cyanobacterial strain, but only marginally affect the O_2 evolution (Vavilin *et al.*, 1999). Furthermore, release of donor-side quenching has previously been hypothesized (Vredenberg, 2008). The data presently available strongly suggest the involvement of a series of events, most likely related to the polarization of molecules/residues on the donor side of PSII (see figure).

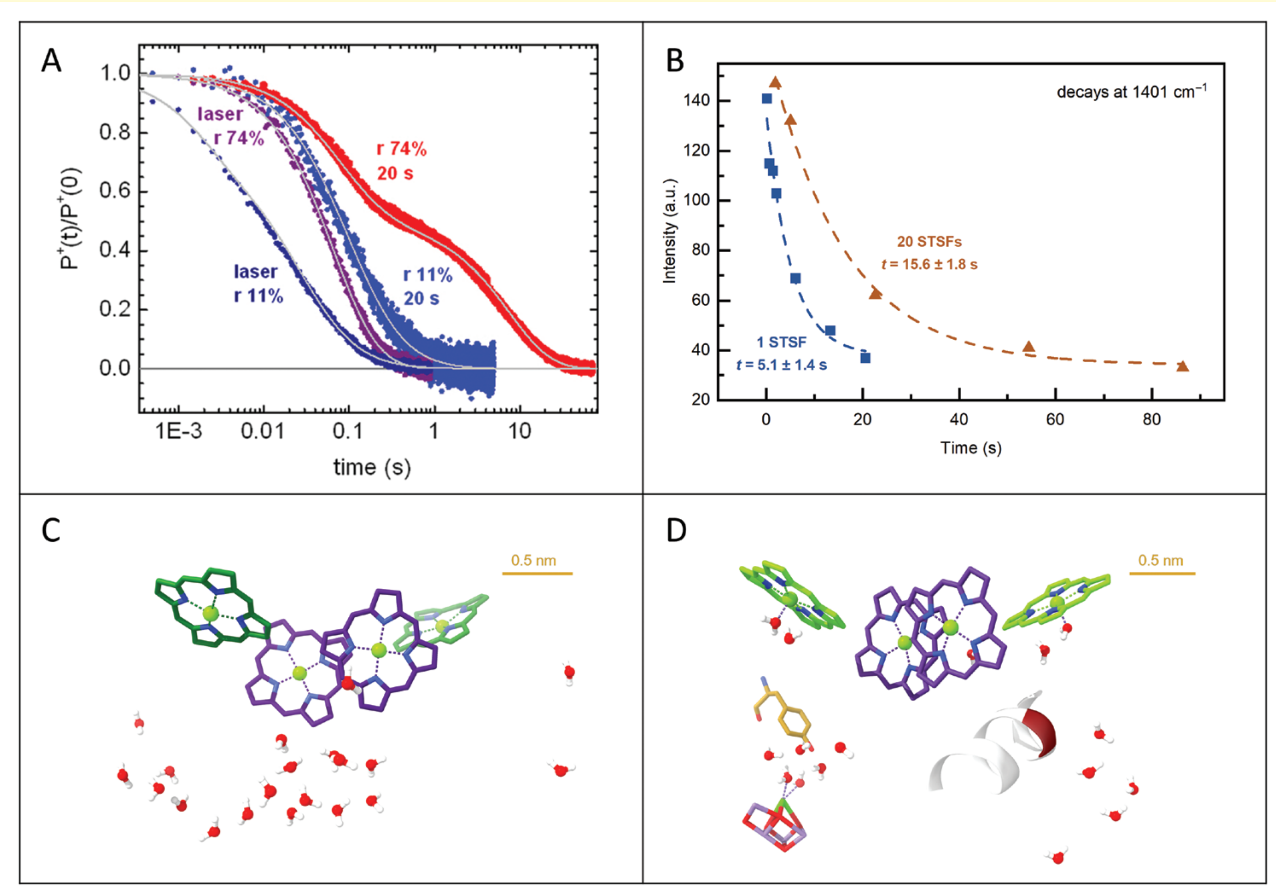

Stabilization of the charge-separated states in bRC and PSII CCs and polarizable groups at the donor sides. (A, B) Pre-illumination dependence of the recombination rates of the charge-separated states in bRC at two different hydration states (r), and (B) in the PSII CC, as described by Malferrari *et al.* (2013) and Sipka *et al.* (2021), respectively. (C, D) Co-factor structures and bound water molecules at the donor side of (C) bRC and (D) PSII, as depicted in Allen *et al.* (2023) and Sipka *et al.* (2022).

at –80 °C Magyar *et al.* (2023), and 0.73 in untreated leaves at room temperature (Laisk and Oja, 2020). Using the data of Joliot and Joliot (1979) from thylakoid membranes, a value of 0.69 would be obtained (the F_v/F_m value is 0.77). Using fast repetition rate flashlets (FRR devices), Prasil *et al.* (2018) could have obtained Y_{p1} and Y_p values of 0.68 and 0.76, respectively, in green algal cells. Note that in all the above cases using STSFs, even at cryogenic temperatures, clear evidence is provided that the first STSF closed all the functional PSII RCs and, in this sense, the efficiency of the RCs to produce stable charge separation could be considered to be 100% in all active centers, i.e. additional STSFs induced no further stable charge separation. For quantum yield determinations more elaborate techniques are needed, for example based on analysis of Chl *a* fluorescence lifetimes (Wientjes *et al.*, 2013), in which the lifetime components of $PSII_C$ (F_1) and the fate of the excitation energy can also be mapped.

In the context of the implicit assumptions used in calculating Y_p, it is interesting to consider the forced-oscillation ChlF technique, which monitors plant responses to sinusoidally modulated light of varying frequency (Nedbal and Lazár, 2021; Lazár *et al.*, 2022). Under these conditions, limitations regarding the variations in the rate constants between different PSII states can be small or negligible, and thus can allow in-depth model calculations to obtain physiologically important parameters of the photosynthetic machinery. The same might hold true for the F_v'/F_m' parameter determined in light-adapted samples (cf. Blankenship, 2021; Lysenko *et al.* 2022), but this requires further careful consideration. It must be emphasized, however, that justification of these assumptions requires further careful investigation. Further, a decreased F_v/F_m (or F_v'/F_m'), for example during photoinhibition of PSII, might be easier to explain with mixed RC populations (Kono *et al.*, 2022), rather than ascribing it to a decreased quantum yield of PSII photochemistry.

By taking into account the large light-induced contributions in ChlF of PSII with closed RCs, it is not surprising that only a relatively small fraction of F_v arises from the Q_A-to-Q_A^-/ $PSII_O$-to-$PSII_C$ transition. It has been pointed out by Mauzerall (1972) that 'the light-induced increases of the effective fluorescence yield in *Chlorella* are too slow to be primary processes in photosynthesis', which argues strongly against the (exclusive and even dominant) role of Q_A^- in F_v. However, since the role of other compounds and/or products in ChlF quenching such as carotenoid triplets (Duysens *et al.*, 1972) or $P_{680}^{\bullet+}$ (Shinkarev and Govindjee, 1993; Akhtar *et al.*, 2022) should not be overlooked, the question requires careful consideration. In this context, it is to be noted that unlike Q_A, these quenchers are generated rather than destroyed upon repeated excitations, and thus do not explain the observed STSF-induced increments in the quasi-stationary levels of ChlF (see also Magyar *et al.*, 2018).

The data presently available suggest that the reduction of Q_A can be held directly responsible for no more than about one-fifth of F_v. Schansker *et al.* (2011) analysed the temperature dependence of the rise times of the fast ChlF of DCMU-poised leaves at cryogenic temperatures and found that the fastest kinetic component, displaying 19.6% of the total amplitude, exhibited very small activation energy (2 kJ mol^{-1}) and thus it was assigned to the primary photochemistry of the RC. A similar amplitude was observed by Magyar *et al.* (2023) in the CC of PSII at −80 °C, an even smaller contribution (~10%) was discerned at 80 K by Sipka *et al.* (2021), and in DCMU-treated CCs of PSII, 2 mM dithionite, which pre-reduces Q_A, decreased the F_v/F_m parameter by only about 23% at 5 °C (Sipka *et al.*, 2021). Finally, Oja and Laisk (2020) found that the immediate rise of ChlF after one STSF in leaves was $1.8F_o$ (with F_v/F_m=0.85, this represents ~14% of F_v). After 40 μs the F_f value increased to $3F_o$ (35% of F_v), with the rise being ascribed to conformational changes in the RC complex.

In Box 3, we outline a proposed physical mechanism of ChlF that is largely based on the well-characterized transition of closed-state to light-adapted state in purple bacterial RC (bRC), which is attributed to complex dielectric relaxation processes. Further, using the recently proposed correlation of this transition with hydrogen-bond networks in purple bacteria, and recalling donor-side dependent ChlF data, we propose that ChlF is largely modulated by electrical polarization events occurring mainly at the donor side of PSII.

Conclusions and perspectives

While several questions remain, we can safely conclude that the interpretation of ChlF must be laid on new foundations. The reduction of Q_A cannot explain the F_o-to-F_m rise, the F_v/F_m parameter cannot be equated with the maximum quantum efficiency of PSII, and the occurrence of excitonic connectivity of PSII units is highly unlikely, and its magnitude certainly cannot be derived from ChlF data. Instead, closed PSII RCs are capable of undergoing light-induced reversible changes, which lead to the gradual formation of a previously unidentified state of PSII, the charge-separated light-adapted (closed) state ($PSII_L$). This state is characterized by an increased stability of charges—a physiologically important change–which is allowed by the structural plasticity of the RC matrix, and affects the basic photophysical and photochemical pathways in the PSII CC. These transitions are most likely determined by the polarizability of hydrogen-bond networks and water molecules at the donor side of PSII; however, the complex dielectric relaxation processes are hindered by the rigidity of the RC matrix, explaining the need for multiple excitations in the $PSII_C$-to-$PSII_L$ transitions.

Despite strong limitations regarding the use of ChlF, we have no doubt that this technique will remain one of the central tools in plant biology and will provide us with much useful information on the photochemical activity and structural and functional dynamics of PSII. Under comparable conditions, and avoiding its pitfalls (Maxwell and Johnson, 2000), ChlF might be used to characterize the photochemical activity of PSII, as evidenced by correlations between the F_v/F_m parameter and, for example, the yield of O_2 evolution or other parameters of photosynthetic activity (Genty *et al.*, 1989; Edwards and Baker, 1993; Hendrickson *et al.*, 2005). However, it is clear that instead of using the 'silver bullet' of the F_v/F_m parameter and equating it with the quantum efficiency of PSII, more careful consideration is required for all the variables of ChlF. Variations in the F_o levels can be cautiously interpreted, as often done in the literature (see Papageorgiou and Govindjee, (2004). In contrast, changes in the F_m level might originate from a range of different effects; to discriminate between them, complementary experiments might help, such as electrochromic absorbance transients (Bailleul *et al.*, 2010), delayed light (Goltsev *et al.*, 2003, 2009), fluorescence lifetimes, and oxygen evolution. Measuring the F_1 level might provide important information on the availability of open RCs, but it should be noted that the flash should be short (1–2 μs) to avoid multiple turnover but nevertheless intense enough to close all the RCs; this might be achieved by using a Xe flash or by FRR flashlets, for example. The novel parameter, half-waiting time ($\Delta\tau_{1/2}$), which can be determined by using a programmable STSF attachment that allows variable time delays between the flashes, holds the promise of characterizing the formation of the light-adapted states.

Finally, we would like to emphasize that, in our opinion, laying the physical mechanism on new foundations does not hamper the use of ChlF, but might rather open new perspectives towards the better understanding of the operation of photosynthetic reaction centers. In this regard, different mutants (for example affecting the protein or lipid compositions of the RCs) and plants from different habitats and with different stress tolerances and possibly with different $\Delta\tau_{1/2}$ values, might be of potential interest for agriculture. Restoring the native $\Delta\tau_{1/2}$ in isolated PSII CCs might uncover important lipid–protein interactions in the structural plasticity of the RC. Advanced spectroscopic methods such as multidimensional spectroscopy techniques applied to the $PSII_{O/C/L}$ states might reveal key factors determining the excitation energy and electron-transfer pathways, and could help explain the physical mechanism of charge stabilization. Stark spectroscopy and modulation of the charge separation with external electric fields and/or rectified intense THz pulses might provide information on the roles of polarization of the RC matrix and dielectric relaxation processes, and on the structural dynamics and protein memory of PSII RCs.

Acknowledgements

The authors are indebted to Drs Szilvia Z. Tóth and László Kovács, and to Professor Douglas Campbell for their critical reading of the manuscript and for helpful comments.

Conflict of interest

The authors declare that they have no conflicts of interest in relation to this work.

Funding

The authors acknowledge support from the Hungarian Ministry of Innovation and Technology, National Research, Development and Innovation Fund (OTKA grants ANN-144012 to PHL and PD-138498 to GS). PHL was also supported by grant 2018-1.2.1-NKP-2018-00009. GG also acknowledges support from the Czech Science Foundation (GA ČR 23-07744S), and the Eötvös Loránd Research Network (ELKH KÖ-36/2021).

Data availability

This paper contains no new experimental data.

References

Ahmadova N, Ho FM, Styring S, Mamedov F. 2017. Tyrozine D oxidation and redox equilibrium in photosystem II. Biochimica et Biophysica Acta - Bioenergetics **1858**, 407–417.

Akhtar P, Sipka G, Han WH, Li XY, Han GY, Shen JR, Garab G, Tan HS, Lambrev PH. 2022. Ultrafast excitation quenching by the oxidized photosystem II reaction center. Journal of Chemical Physics **156**, 145101.

Allen JP, Chamberlain KD, Williams JC. 2023. Identification of amino acid residues in a proton release pathway near the bacteriochlorophyll dimer in reaction centers from *Rhodobacter sphaeroides*. Photosynthesis Research **155**, 23–34.

Andréasson U, Andréasson LE. 2003. Characterization of a semi-stable, charge-separated state in reaction centers from *Rhodobacter sphaeroides*. Photosynthesis Research **75**, 223–233.

Bailleul B, Cardol P, Breyton C, Finazzi G. 2010. Electrochromism: a useful probe to study algal photosynthesis. Photosynthesis Research **106**, 179–189.

Barber J. 2004. Engine of life and big bang of evolution: a personal perspective. Photosynthesis Research **80**, 137–155.

Barber J, Morris E, Buchel C. 2000. Revealing the structure of the photosystem II chlorophyll binding proteins, CP43 and CP47. Biochimica et Biophysica Acta - Bioenergetics **1459**, 239–247.

Blankenship RE. 2021. Molecular mechanisms of photosynthesis, 3rd edn. Chichester, UK: Wiley.

Butler WL. 1978. Energy-distribution in photo-chemical apparatus of photosynthesis. Annual Review of Plant Physiology and Plant Molecular Biology **29**, 345–378.

Caffarri S, Broess K, Croce R, van Amerongen H. 2011. Excitation energy transfer and trapping in higher plant photosystem II complexes with different antenna sizes. Biophysical Journal **100**, 2094–2103.

Campbell D, Hurry V, Clarke AK, Gustafsson P, Oquist G. 1998. Chlorophyll fluorescence analysis of cyanobacterial photosynthesis and acclimation. Microbiology and Molecular Biology Reviews **62**, 667–683.

Cardona T, Sedoud A, Cox N, Rutherford AW. 2012. Charge separation in photosystem II: a comparative and evolutionary overview. Biochimica et Biophysica Acta - Bioenergetics **1817**, 26–43.

Christophorov L, Holzwarth A, Kharkyanen V. 2003. Conformational regulation in single molecule reactions. Ukrainian Journal of Physics **48**, 672–680.

Coe J, Kupitz C, Basu S, Conrad CE, Roy-Chowdhury S, Fromme R, Fromme P. 2015. Crystallization of photosystem II for time-resolved structural studies using an X-ray free electron laser. In: Shukla AK. ed. Methods in enzymology, vol. **557**. Cambridge, MA: Academic Press, 459–482.

Croce R, van Amerongen H. 2014. Natural strategies for photosynthetic light harvesting. Nature Chemical Biology **10**, 492–501.

Cseh Z, Rajagopal S, Tsonev T, Busheva M, Papp E, Garab G. 2000. Thermooptic effect in chloroplast thylakoid membranes. Thermal and light stability of pigment arrays with different levels of structural complexity. Biochemistry **39**, 15250–15257.

Cser K, Vass I. 2007. Radiative and non-radiative charge recombination pathways in photosystem II studied by thermoluminescence and chlorophyll fluorescence in the cyanobacterium *Synechocystis* 6803. Biochimica et Biophysica Acta - Bioenergetics **1767**, 233–243.

Dau H, Sauer K. 1992. Electric-field effect on the picosecond fluorescence of photosystem II and its relation to the energetics and kinetics of primary charge separation. Biochimica et Biophysica Acta - Bioenergetics **1102**, 91–106.

Delosme R. 1967. Studies on the induction of fluorescence in green algae and chloroplasts under intense illumination. Biochimica et Biophysica Acta - Bioenergetics **143**, 108–128. [In French.]

Delosme R, Joliot P. 2002. Period four oscillations in chlorophyll *a* fluorescence. Photosynthesis Research **73**, 165–168.

Deshmukh SS, Williams JC, Allen JP, Kalman L. 2011. Light-induced conformational changes in photosynthetic reaction centers: dielectric relaxation in the vicinity of the dimer. Biochemistry **50**, 340–348.

Diner BA, Bautista JA, Nixon PJ, Berthomieu C, Hienerwadel R, Britt RD, Vermaas WFJ, Chisholm DA. 2004. Coordination of proton and electron transfer from the redox-active tyrosine, Y_Z, of photosystem II and examination of the electrostatic influence of oxidized tyrosine, $Y_D^{\bullet}(H^+)$. Physical Chemistry Chemical Physics **6**, 4844–4850.

Duysens L, Sweers H. 1963. Mechanism of two photochemical reactions in algae as studied by means of fluorescence. In: Japanese Society of Plant

Physiologists. eds. Studies on microalgae and photosynthetic bacteria.. Tokyo: University of Tokyo Press, 353–372.

Duysens LNM, van der Schatte-Olivier TE, den Haan GA. 1972. Light induced quenching of the yield of chlorophyll *a*2 fluorescence, with microsecond back reaction stimulated by oxygen. In: Schenck GO, ed. Progress in photobiology, Proceedings of the VI International Congress on Photobiology held in Bochum 1972, Abstract No. 277. Berlin: Deutsche Gesellschaft für Lichtforschung.

Edwards GE, Baker NR. 1993. Can CO_2 assimilation in maize leaves be predicted accurately from chlorophyll fluorescence analysis? Photosynthesis Research **37**, 89–102.

France LL, Geacintov NE, Breton J, Valkunas L. 1992. The dependence of the degrees of sigmoidicities of fluorescence induction curves in spinach chloroplasts on the duration of actinic pulses in pump-probe experiments. Biochimica et Biophysica Acta - Bioenergetics **1101**, 105–119.

Genty B, Briantais JM, Baker NR. 1989. The relationship between the quantum yield of photosynthetic electron transport and quenching of chlorophyll fluorescence. Biochimica et Biophysica Acta – General Subjects **990**, 87–92.

Goltsev V, Zaharieva I, Chernev P, Strasser RJ. 2009. Delayed fluorescence in photosynthesis. Photosynthesis Research **101**, 217–232.

Goltsev V, Zaharieva I, Lambrev P, Yordanov I, Strasser R. 2003. Simultaneous analysis of prompt and delayed chlorophyll *a* fluorescence in leaves during the induction period of dark to light adaptation. Journal of Theoretical Biology **225**, 171–183.

Gorbunov MY, Falkowski PG. 2022. Using chlorophyll fluorescence to determine the fate of photons absorbed by phytoplankton in the world's oceans. Annual Review of Marine Science **14**, 213–238.

Goushcha AO, Holzwarth AR, Kharkyanen VN. 1999. Self-regulation phenomenon of electron-conformational transitions in biological electron transfer under nonequilibrium conditions. Physical Review E **59**, 3444–3452.

Goushcha AO, Kharkyanen VN, Scott GW, Holzwarth AR. 2000. Self-regulation phenomena in bacterial reaction centers. I. General theory. Biophysical Journal **79**, 1237–1252.

Goushcha AO, Manzo AJ, Scott GW, Christophorov LN, Knox PP, Barabash YM, Kapoustina MT, Berezetska NM, Kharkyanen VN. 2003. Self-regulation phenomena applied to bacterial reaction centers: 2. Nonequilibrium adiabatic potential: Dark and light conformations revisited. Biophysical Journal **84**, 1146–1160.

Hendrickson L, Forster B, Pogson BJ, Chow WS. 2005. A simple chlorophyll fluorescence parameter that correlates with the rate coefficient of photoinactivation of photosystem II. Photosynthesis Research **84**, 43–49.

Horton P. 2012. Optimization of light harvesting and photoprotection: molecular mechanisms and physiological consequences. Philosophical Transactions of the Royal Society B - Biological Sciences **367**, 3455–3465.

Joliot P, Joliot A. 1979. Comparative study of the fluorescence yield and of the C550 absorption change at room temperature. Biochimica et Biophysica Acta - Bioenergetics **546**, 93–105.

Kalaji HM, Schansker G, Ladle RJ, *et al*. 2014. Frequently asked questions about *in vivo* chlorophyll fluorescence: practical issues. Photosynthesis Research **122**, 121–158.

Kleinfeld D, Okamura MY, Feher G. 1984. Electron-transfer kinetics in photosynthetic reaction centers cooled to cryogenic temperatures in the charge-separated state - Evidence for light-induced structural changes. Biochemistry **23**, 5780–5786.

Knox PP, Garab G. 1982. The effect of a permanent electric field on thermoluminescence of chloroplasts. Photochemistry and Photobiology **35**, 733–736.

Kono M, Miyata K, Matsuzawa S, Noguchi T, Oguchi R, Suzuki Y, Terashima I. 2022. Mixed population hypothesis of the active and inactive PSII complexes opens a new door for photoinhibition and fluorescence studies: an ecophysiological perspective. Functional Plant Biology **49**, 917–925.

Laisk A, Oja V. 2020. Variable fluorescence of closed photochemical reaction centers. Photosynthesis Research **143**, 335–346.

Lazár D, Pospíšil P. 1999. Mathematical simulation of chlorophyll *a* fluorescence rise measured with 3-(3´,4´-dichlorophenyl)-1,1-dimethylurea-treated barley leaves at room and high temperatures. European Biophysics Journal **28**, 468–477.

Lazár D, Niu Y, Nedbal L. 2022. Insights on the regulation of photosynthesis in pea leaves exposed to oscillating light. Journal of Experimental Botany **73**, 6380–6393.

Loayza H, Moya I, Quiroz R, Ounis A, Goulas Y. 2023. Active and passive chlorophyll fluorescence measurements at canopy level on potato crops. Evidence of similitude of diurnal cycles of apparent fluorescence yields. Photosynthesis Research **155**, 271–288.

Lysenko V, Vishnu DR, Kumar Singh R, *et al*. 2022. Chlorophyll fluorometry in evaluating photosynthetic performance: key limitations, possibilities, perspectives and alternatives. Physiology and Molecular Biology of Plants **28**, 2041–2056.

Magyar M, Akhtar P, Sipka G, Han W, Li X, Han G, Shen JR, Lambrev PH, Garab G. 2022. Dependence of the rate-limiting steps in the dark-to-light transition of photosystem II on the lipidic environment of the reaction center. Photosynthetica **60**, 147–156.

Magyar M, Sipka G, Han WH, Li XY, Han GY, Shen JR, Lambrev PH, Garab G. 2023. Characterization of the rate-limiting steps in the dark-to-light transitions of closed photosystem II: temperature dependence and invariance of waiting times during multiple light reactions. International Journal of Molecular Sciences **24**, 94.

Magyar M, Sipka G, Kovacs L, Ughy B, Zhu QJ, Han GY, Spunda V, Lambrev PH, Shen JR, Garab G. 2018. Rate-limiting steps in the dark-to-light transition of photosystem II – revealed by chlorophyll-*a* fluorescence induction. Scientific Reports **8**, 2755.

Malferrari M, Mezzetti A, Francia F, Venturoli G. 2013. Effects of dehydration on light-induced conformational changes in bacterial photosynthetic reaction centers probed by optical and differential FTIR spectroscopy. Biochimica et Biophysica Acta - Bioenergetics **1827**, 328–339.

Marcus RA, Sutin N. 1985. Electron transfers in chemistry and biology. Biochimica et Biophysica Acta – Reviews on Bioenergetics **811**, 265–322.

Mauzerall D. 1972. Light-induced fluorescence changes in *Chlorella*, and the primary photoreactions for the production of oxygen. Proceedings of the National Academy of Sciences, USA **69**, 1358–1362.

Maxwell K, Johnson GN. 2000. Chlorophyll fluorescence—a practical guide. Journal of Experimental Botany **51**, 659–668.

Miloslavina Y, Szczepaniak M, Muller MG, Sander J, Nowaczyk M, Rogner M, Holzwarth AR. 2006. Charge separation kinetics in intact photosystem II core particles is trap-limited. A picosecond fluorescence study. Biochemistry **45**, 2436–2442.

Moise N, Moya I. 2004. Correlation between lifetime heterogeneity and kinetics heterogeneity during chlorophyll fluorescence induction in leaves: 1. Mono-frequency phase and modulation analysis reveals a conformational change of a PSII pigment complex during the IP thermal phase. Biochimica et Biophysica Acta - Bioenergetics **1657**, 33–46.

Morin P. 1964. Études des cinétiques de fluorescence de la chlorophylle in vivo, dans les premiers instants qui suivent le début de l'illumination. Journal de Chimie Physique **61**, 674–680.

Muh F, Plockinger M, Renger T. 2017. Electrostatic asymmetry in the reaction center of photosystem II. Journal of Physical Chemistry Letters **8**, 850–858.

Murchie EH, Harbinson J. 2014. Non-photochemical fluorescence quenching across scales: from chloroplasts to plants to communities. In: Demmig-Adams B, Garab G, Adams **III** W, Govindjee, eds. Non-photochemical quenching and energy dissipation in plants, algae and cyanobacteria. Dordrecht: Springer Netherlands, 553–582.

Nakamura S, Noguchi T. 2015. Infrared detection of a proton released from tyrosine Y_D to the bulk upon its photo-oxidation in photosystem II. Biochemistry **54**, 5045–5053.

Nakanishi M, Sokolov AP. 2015. Dielectric spectroscopy of hydrated biomacromolecules. In: Raicu V, Feldman Y, eds. Dielectric relaxation in biological systems: physical principles, methods, and applications. Oxford, UK: Oxford University Press, 248–275.

Nedbal L, Lazár D. 2021. Photosynthesis dynamics and regulation sensed in the frequency domain. Plant Physiology **187**, 646–661.

Nelson N, Junge W. 2015. Structure and energy transfer in photosystems of oxygenic photosynthesis. Annual Review of Biochemistry **84**, 659–683.

Neubauer C, Schreiber U. 1987. The polyphasic rise of chlorophyll fluorescence upon onset of strong continuous illumination. 1. Saturation characteristics and partial control by the photosystem-II acceptor side. Zeitschrift Für Naturforschung C **42**, 1246–1254.

Novoderezhkin VI, Romero E, Dekker JP, van Grondelle R. 2011. Multiple charge-separation pathways in photosystem II: modeling of transient absorption kinetics. ChemPhysChem **12**, 681–688.

Oja V, Laisk A. 2020. Time- and reduction-dependent rise of photosystem II fluorescence during microseconds-long inductions in leaves. Photosynthesis Research **145**, 209–225.

Oxborough K, Baker NR. 1997. Resolving chlorophyll *a* fluorescence images of photosynthetic efficiency into photochemical and non-photochemical components – calculation of qP and Fv-/Fm-; without measuring Fo. Photosynthesis Research **54**, 135–142.

Papageorgiou GC, Govindjee. eds. 2004. Chlorophyll a fluorescence. A signature of photosynthesis. Advances in photosynthesis and respiration, vol. **19**. Dordrecht, The Netherlands: Springer.

Pettersen EF, Goddard TD, Huang CC, Meng EC, Couch GS, Croll TI, Morris JH, Ferrin TE. 2021. UCSF ChimeraX: structure visualization for researchers, educators, and developers. Protein Science **30**, 70–82.

Prasil O, Kolber ZS, Falkowski PG. 2018. Control of the maximal chlorophyll fluorescence yield by the Q_B binding site. Photosynthetica **56**, 150–162.

Romero E, Novoderezhkin VI, van Grondelle R. 2017. Quantum design of photosynthesis for bio-inspired solar-energy conversion. Nature **543**, 355–365.

Ruban AV, Wilson S. 2021. The mechanism of non-photochemical quenching in plants: localization and driving forces. Plant & Cell Physiology **62**, 1063–1072.

Santabarbara S, Villafiorita Monteleone F, Remelli W, Rizzo F, Menin B, Casazza AP. 2019. Comparative excitation–emission dependence of the F_V/F_M ratio in model green algae and cyanobacterial strains. Physiologia Plantarum **166**, 351–364.

Schansker G, Toth SZ, Kovacs L, Holzwarth AR, Garab G. 2011. Evidence for a fluorescence yield change driven by a light-induced conformational change within photosystem II during the fast chlorophyll *a* fluorescence rise. Biochimica et Biophysica Acta- Bioenergetics **1807**, 1032–1043.

Schansker G, Toth SZ, Strasser RJ. 2005. Methylviologen and dibromothymoquinone treatments of pea leaves reveal the role of photosystem I in the Chl *a* fluorescence rise OJIP. Biochimica et Biophysica Acta - Bioenergetics **1706**, 250–261.

Schreiber U. 2023. Light-induced changes of far-red excited chlorophyll fluorescence: further evidence for variable fluorescence of photosystem I *in vivo*. Photosynthesis Research **155**, 247–270.

Shen JR. 2015. The structure of photosystem II and the mechanism of water oxidation in photosynthesis. Annual Review of Plant Biology **66**, 23–48.

Shevela D, Kern JF, Govindjee G, Messinger J. 2023. Solar energy conversion by photosystem II: principles and structures. Photosynthesis Research **156**, 279–307.

Shibata Y, Nishi S, Kawakami K, Shen JR, Renger T. 2013. Photosystem II does not possess a simple excitation energy funnel: time-resolved fluorescence spectroscopy meets theory. Journal of the American Chemical Society **135**, 6903–6914.

Shinkarev VP, Govindjee. 1993. Insight into the relationship of chlorophyll-a fluorescence yield to the concentration of its natural quenchers in oxygenic photosynthesis. Proceedings of the National Academy of Sciences, USA **90**, 7466–7469.

Shlyk-Kerner O, Samish I, Kaftan D, Holland N, Sai PS, Kless H, Scherz A. 2006. Protein flexibility acclimatizes photosynthetic energy conversion to the ambient temperature. Nature **442**, 827–830.

Sipka G, Magyar M, Mezzetti A, *et al*. 2021. Light-adapted charge-separated state of photosystem II: structural and functional dynamics of the closed reaction center. The Plant Cell **33**, 1286–1302.

Sipka G, Muller P, Brettel K, *et al*. 2019. Redox transients of P680 associated with the incremental chlorophyll-*a* fluorescence yield rises elicited by a series of saturating flashes in diuron-treated photosystem II core complex of *Thermosynechococcus vulcanus*. Physiologia Plantarum **166**, 22–32.

Sipka G, Nagy L, Magyar M, Akhtar P, Shen JR, Holzwarth AR, Lambrev PH, Garab G. 2022. Light-induced reversible reorganizations in closed Type II reaction centre complexes: physiological roles and physical mechanisms. Open Biology **12**, 220297.

Stirbet A. 2013. Excitonic connectivity between photosystem II units: what is it, and how to measure it? Photosynthesis Research **116**, 189–214.

Stirbet A, Govindjee. 2011. On the relation between the Kautsky effect (chlorophyll *a* fluorescence induction) and photosystem II: basics and applications of the OJIP fluorescence transient. Journal of Photochemistry and Photobiology B: Biology **104**, 236–257.

Stirbet A, Govindjee. 2012. Chlorophyll *a* fluorescence induction: a personal perspective of the thermal phase, the J–I–P rise. Photosynthesis Research **113**, 15–61.

Strasser RJ, Tsimilli-Michael M, Srivastava A. 2004. Analysis of the chlorophyll *a* fluorescence transient. In: Papageorgiou GC, Govindjee, eds. Chlorophyll a fluorescence. A signature of photosynthesis. Advances in photosynthesis and respiration, vol. **19**. Dordrecht, The Netherlands: Springer, 321–362.

Suga M, Akita F, Yamashita K, *et al*. 2019. An oxyl/oxo mechanism for oxygen–oxygen coupling in PSII revealed by an X-ray free-electron laser. Science **366**, 334–338.

Szczepaniak M, Sander J, Nowaczyk M, Muller MG, Rogner M, Holzwarth AR. 2009. Charge separation, stabilization, and protein relaxation in photosystem II core particles with closed reaction center. Biophysical Journal **96**, 621–631.

Tóth SZ, Schansker G, Strasser RJ. 2007. A non-invasive assay of the plastoquinone pool redox state based on the OJIP-transient. Photosynthesis Research **93**, 193–203.

Treves H, Raanan H, Kedem I, *et al*. 2016. The mechanisms whereby the green alga *Chlorella ohadii*, isolated from desert soil crust, exhibits unparalleled photodamage resistance. New Phytologist **210**, 1229–1243.

Tyystjarvi E, Vass I. 2004. Light emission as a probe of charge separation and recombination in the photosynthetic apparatus: relation of prompt fluorescence to delayed light emission and thermoluminescence. In: Papageorgiou GC, Govindjee, eds. Chlorophyll a fluorescence. A signature of photosynthesis. Advances in photosynthesis and respiration, vol. **19**. Dordrecht, The Netherlands: Springer, 363–388.

Umena Y, Kawakami K, Shen JR, Kamiya N. 2011. Crystal structure of oxygen-evolving photosystem II at a resolution of 1.9 Å. Nature **473**, 55–60.

van der Weij-de Wit CD, Dekker JP, van Grondelle R, van Stokkum IHM. 2011. Charge separation is virtually irreversible in photosystem II core complexes with oxidized primary quinone acceptor. Journal of Physical Chemistry A **115**, 3947–3956.

Vavilin DV, Ermakova-Gerdes SY, Keilty AT, Vermaas WF. 1999. Tryptophan at position 181 of the D2 protein of photosystem II confers quenching of variable fluorescence of chlorophyll: implications for the mechanism of energy-dependent quenching. Biochemistry **38**, 14690–14696.

Vredenberg WJ. 2008. Analysis of initial chlorophyll fluorescence induction kinetics in chloroplasts in terms of rate constants of donor side quenching release and electron trapping in photosystem II. Photosynthesis Research **96**, 83–97.

Vredenberg W. 2011. Kinetic analyses and mathematical modeling of primary photochemical and photoelectrochemical processes in plant photosystems. Biosystems **103**, 138–151.

Vredenberg W. 2015. A simple routine for quantitative analysis of light and dark kinetics of photochemical and non-photochemical quenching of chlorophyll fluorescence in intact leaves. Photosynthesis Research **124**, 87–106.

Wientjes E, van Amerongen H, Croce R. 2013. Quantum yield of charge separation in photosystem II: functional effect of changes in the antenna size upon light acclimation. Journal of Physical Chemistry B **117**, 11200–11208.

Yang SJ, Arsenault EA, Orcutt K, Iwai M, Yoneda Y, Fleming GR. 2022. From antenna to reaction center: pathways of ultrafast energy and charge transfer in photosystem II. Proceedings of the National Academy of Sciences, USA **119**, e2208033119.

Yao JN, Sun DW, Cen HY, Xu HX, Weng HY, Yuan F, He Y. 2018. Phenotyping of Arabidopsis drought stress response using kinetic chlorophyll fluorescence and multicolor fluorescence imaging. Frontiers in Plant Science **9**, 603.

Yoneda Y, Katayama T, Nagasawa Y, Miyasaka H, Umena Y. 2016. Dynamics of excitation energy transfer between the subunits of photosystem II dimer. Journal of the American Chemical Society **138**, 11599–11605.

Zabret J, Bohn S, Schuller SK, *et al*. 2021. Structural insights into photosystem II assembly. Nature Plants **7**, 524–538.